Neuron
Article

A Transcription Factor Network Coordinates Attraction, Repulsion, and Adhesion Combinatorially to Control Motor Axon Pathway Selection

Aref Arzan Zarin,[1,2] Jamshid Asadzadeh,[1,2] Karsten Hokamp,[1] Daniel McCartney,[1] Long Yang,[3] Greg J. Bashaw,[3] and Juan-Pablo Labrador[1,2,*]
[1]Smurfit Institute of Genetics, Trinity College Dublin, Dublin 2, Ireland
[2]Institute of Neuroscience, Trinity College Dublin, Dublin 2, Ireland
[3]Department of Neuroscience, Perelman School of Medicine, University of Pennsylvania, Philadelphia, PA 19104, USA
*Correspondence: labradoj@tcd.ie
http://dx.doi.org/10.1016/j.neuron.2014.01.038

SUMMARY

Combinations of transcription factors (TFs) instruct precise wiring patterns in the developing nervous system; however, how these factors impinge on surface molecules that control guidance decisions is poorly understood. Using mRNA profiling, we identified the complement of membrane molecules regulated by the homeobox TF Even-skipped (Eve), the major determinant of dorsal motor neuron (dMN) identity in *Drosophila*. Combinatorial loss- and gain-of-function genetic analyses of Eve target genes indicate that the integrated actions of attractive, repulsive, and adhesive molecules direct *eve*-dependent dMN axon guidance. Furthermore, combined misexpression of Eve target genes is sufficient to partially restore CNS exit and can convert the guidance behavior of interneurons to that of dMNs. Finally, we show that a network of TFs, comprised of *eve, zfh1*, and *grain,* induces the expression of the Unc5 and Beaten-path guidance receptors and the Fasciclin 2 and Neuroglian adhesion molecules to guide individual dMN axons.

INTRODUCTION

How axons follow specific paths depends on receptors expressed on their membranes that elicit a coordinated response to extracellular signals. Numerous guidance receptors and cell adhesion molecules (CAMs) have been discovered in the last two decades and they are generally classified into four nonexclusive categories as mediators of long-range or contact-mediated attraction or repulsion (Kolodkin and Tessier-Lavigne, 2011). Accordingly, as axons navigate, they respond to several cues of different nature in a complex extracellular environment to choose their correct path (Tessier-Lavigne and Goodman, 1996). However, it remains unclear how the combined expression and function of different receptors and CAMs controls the pathfinding decisions of individual neurons (Pecot et al., 2013) or how it is transcriptionally regulated.

Combinatorial codes of transcription factors (TFs) are essential for axonal pathway selection (Dasen and Jessell, 2009; Thor and Thomas, 1997; Tsuchida et al., 1994). It is generally assumed that transcriptional codes regulate the expression of guidance receptors, although few functional links have been established (Bonanomi and Pfaff, 2010; Zarin et al., 2014). For example, Zic2, a determinant for the retinal ganglion cells whose axons do not cross the optic chiasm, regulates the expression of the EphB1 receptor (Herrera et al., 2003). In addition, molecules that act together to control specific aspects of neuronal function as the battery of genes responsible for the synthesis, packaging, and degradation of acetylcholine as well as choline reuptake in motoneurons are all regulated by a single TF, UNC-3 in *C. elegans* (Kratsios et al., 2012). Thus, available data support a model in which transcriptional regulators that act as determinants for specific subsets of neurons coordinate the expression of several molecular programs to impart wiring specificity and to confer specific functional properties.

The *Drosophila* neuromuscular system is particularly well suited for an exploration of the functional relationships between TF determinants of motor neuron identity and the cell surface molecules that direct wiring specificity. It consists of a segmentally reiterated arrangement of 30 muscles innervated by 36 motoneurons that fasciculate together into three main branches, the transverse nerve (TN), intersegmental nerve (ISN), and the segmental nerve (SN) (Landgraf and Thor, 2006). The pioneer neurons for the ISN, the aCC and RP2 motoneurons, fasciculate, project away from the CNS, navigate through the muscle field, and innervate their dorsal muscle targets (Figure 1B). The homeodomain TF Even-skipped (Eve) largely determines the specific guidance characteristics of the aCC and RP2 dorsal motoneurons (dMNs) (Doe et al., 1988; Fujioka et al., 2003; Landgraf et al., 1999). When *eve* is absent in dMNs, they no longer project away from the CNS (Figure 1C) and the ISN stops short of its most dorsal target muscles (Fujioka et al., 2003; Landgraf et al., 1999). *eve* regulates the expression of the guidance receptors Unc-5 (Labrador et al., 2005); however, *unc-5* has a relatively mild guidance phenotype when compared to *eve* mutants (Labrador et al., 2005). The fact that the *eve* mutant phenotype is so much stronger than phenotypes observed in guidance receptor and CAM mutants suggests that *eve* is likely to control several different

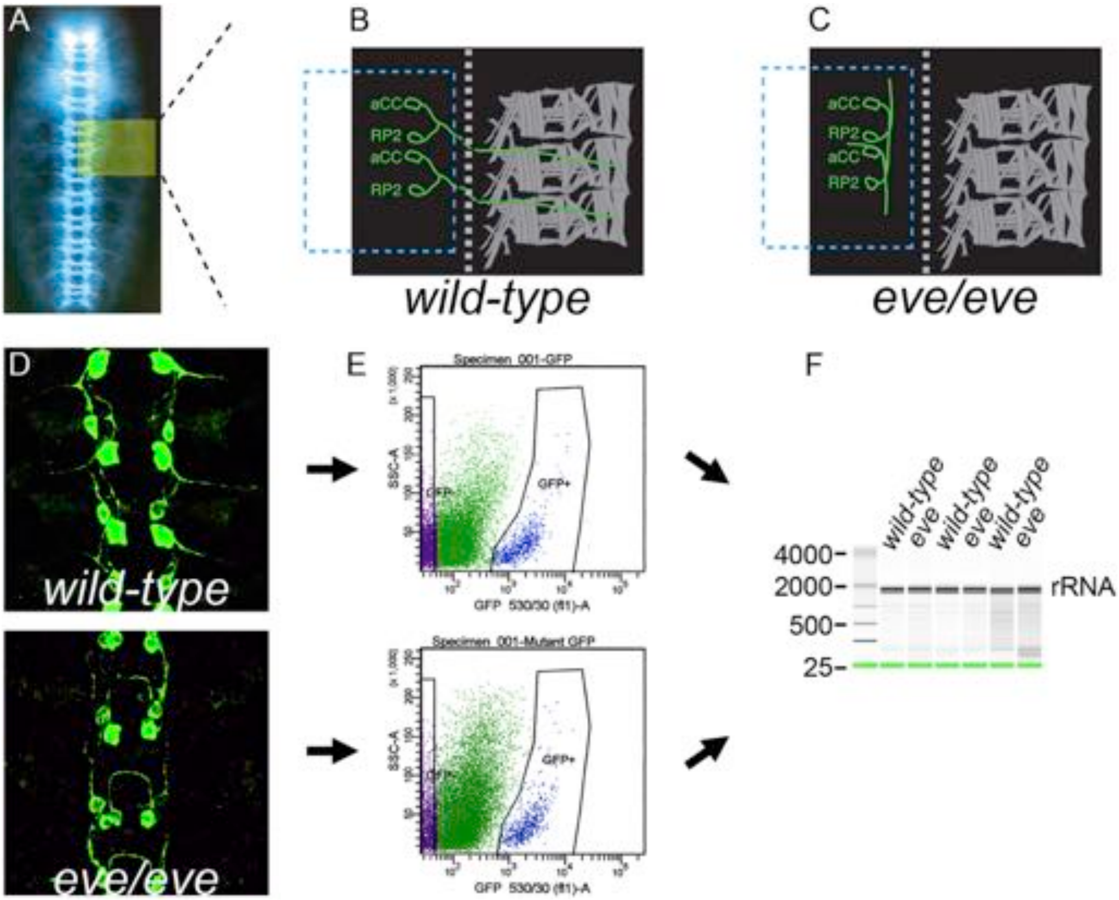

Figure 1. Sorting of Wild-Type and *eve* Mosaic aCC and RP2 Motor Neurons Followed by Total RNA Extraction and Microarray Hybridization

(A) Diagram representing the relative position of aCC and RP2 motoneurons in a *Drosophila* embryo nerve cord with laterally projecting motoneurons; the area shaded in yellow is represented in cartoons (B) and (C).

(B and C) Schematic diagrams illustrating magnified views of (A) inset in wild-type (B) and *eve* mosaic embryos where *eve* is only absent in aCC, RP2, and pCC neurons (C). In wild-type embryos, aCC and RP2 axons exit laterally and innervate their most dorsal target muscles, whereas in *eve* mosaic animals, a majority of them fail to exit the CNS.

(D) Stage 13 embryos carrying RN2 driving GFP either in a wild-type background (top) or an *eve* mosaic background (bottom).

(E) Embryos were dissociated and GFP-positive aCC and RP2 neurons were FACS sorted based on their fluorescence.

(F) Total RNA was extracted from FACS-sorted cells and analyzed for quality by electrophoresis based on the presence of the double band of ribosomal RNA (rRNA).

guidance pathways that work together to control the correct trajectory of dorsal motor axons.

We now provide evidence that *eve* orchestrates the expression of several axon guidance pathways in dMNs and propose that *eve* together with *zfh1* and *grn* comprise a transcriptional code required for the combinatorial expression of these guidance molecules. Using mRNA profiling of fluorescence-activated cell-sorted (FACS) wild-type and *eve* mutant dMNs in microarrays, followed by in vivo single-cell resolution expression analyses, we show that *eve* regulates the Beat Ia and Unc-5 receptors and the adhesive CAMs Fas2 and Nrg. These molecules are all expressed in dMNs as their axons start to navigate toward the muscle field in wild-type dMNs, but their mRNA levels are significantly reduced or undetectable in *eve* mutant dMNs. The TFs Grn and Zfh1 regulate overlapping subsets of these guidance molecules in dMNs. Individual loss of function of these guidance genes generally result in mild guidance phenotypes; however, their combined elimination shows a progressively stronger phenotype in which the ISN stops short of its targets and aCC and RP2 fail to exit the CNS, as is observed in *eve* mutants. Combinatorial reintroduction of these molecules in *eve* mutants can lead to CNS exit. This effect is achieved through the combination of different activities: (1) a repulsive action of Unc-5 directing aCC and RP2 away from the midline Netrin source, (2) the attractive effect of the Beat-Ia receptor toward the CNS exit points, and (3) fasciculation of aCC and RP2 mediated by the Nrg and Fas2 CAMs. Additionally, we show that *eve* can induce the expression of *Fas2*, *beat Ia*, *nrg*, and *unc-5* in EW commissural interneurons and redirect their axons away from the midline toward the muscle field. This effect is replicated by the combined expression of the *eve*-regulated guidance genes. Finally, we show that *zfh1* can also induce the expression of

Fas2, *beat Ia*, and *unc-5* and that the combined expression of *eve* and *zfh-1* or *grn* induces a stronger expression of the guidance genes in EW neurons and promotes increased exit of their axons. Thus, the dorsal motoneuron determinant *eve* partially controls the response of individual motor axons by regulating the precise expression of receptors and CAMs and can cooperatively regulate their levels together with *grn* and *zfh1* to integrate their different responses (attraction, repulsion, and adhesion) into the correct guidance choice.

RESULTS

Comparative mRNA Profiling of Wild-Type and *eve* Mutant Dorsal Motoneurons Identifies Multiple *eve*-Regulated Genes

To determine transcriptional profiles of individual motoneurons, we developed a system to isolate aCC, RP2, and pCC neurons. We used the UAS/Gal4 system with the *RN2Gal4* driver expressing *mCD8GFP* in wild-type or *eve* mosaic mutant embryos (Figure 1D), synchronized and aged to late stage 12, at onset of axon guidance. To overcome the early patterning effects due to *eve* loss of function, we used *eve* mosaic mutants, in which *eve* function is exclusively eliminated in aCC, pCC, and RP2 neurons (Fujioka et al., 2003). We purified GFP-positive dMNs by FACS (Figure 1E), extracted total RNA (Figure 1F), and labeled cRNA was hybridized to GeneChip *Drosophila* Genome 2.0 Arrays. A confirmation of microarray results by in situ hybridization and confocal imaging allowed us to achieve differential transcriptional profiles with single-cell resolution.

We identified 561 genes differentially expressed between wild-type and *eve* mutants displaying a false discovery rate (FDR) <0.05 and at least a 1.5-fold expression-level difference. Most of the identified genes showed downregulation in *eve* mutants. Gene Ontology (GO) of differentially expressed genes was analyzed and manually annotated. Based on biological processes, 227 genes were categorized into 55 clusters. Among the top 10% of clusters identified were ‘‘Neurological System Process’’ and ‘‘Neuron Projection Morphogenesis,’’ where GO terms ‘‘Axon Guidance’’ and ‘‘Axonogenesis’’ were included (Table S1 and Figures S1 and S2 available online). Microarray results were confirmed by in situ hybridization for genes in the top two enriched neuronal GO categories in wild-type and *eve* mosaic mutants, where the cell bodies of aCC and RP2 dMNs were also labeled by protein markers (*RN2Gal4* driving *UAS-taumyc*) (Figure 2 and Figure S2). This allowed us to quantify the changes in their mRNA levels with single-cell resolution. All of the genes in these categories (13) except *synj* (Figure S2) showed significant reduction ($p < 0.001$) of mRNA signal in *eve* mutant dMNs. A comparison of the genes identified in our screen and a previous study in which genome-wide *eve* binding was examined through DamID (Pym et al., 2006) reveals that Eve can bind within 2 kb of at least 10% of the genes we identified (T. Southall, R. Baines, and A. Brand, personal communication).

Eve Regulates Attraction, Repulsion, and Adhesion

We focused on genes coding for membrane molecules annotated with axonal-related processes differentially expressed between wild-type and *eve* mutant aCC and RP2 dMNs and identified several not previously known to be regulated by *eve*: Beat Ia (Fambrough and Goodman, 1996), an attractive receptor (Siebert et al., 2009) for Sidestep (Sink et al., 2001) (Figures 2D–2F), the CAM Neuroglian (Nrg), a *Drosophila* homolog of the vertebrate L1CAM (Bieber et al., 1989) (Figures 2G–2I), and Fasciclin 2 (Fas2) (Grenningloh et al., 1991), the *Drosophila* homolog of NCAM (Figures 2A–2C). Together with *Drosophila* Unc-5, a repulsive receptor for Netrins (Harris et al., 1996; Mitchell et al., 1996) that has been shown to be regulated by *eve* (Labrador et al., 2005) (Figures 2J–2L), they all belong to the immunoglobulin superfamily and may act together to mediate guidance downstream of *eve*. We analyzed the mRNA expression of these genes by fluorescent in situ hybridization in wild-type and *eve* mutant aCC and RP2 dMNs and quantified the fluorescent signal (Figures 2C, 2F, 2I, and 2L). While all of these genes are expressed in dMNs in wild-type (*eve*/+) embryos at stage 15 (Figures 2A, 2D, 2G, and 2J), their mRNA levels are significantly reduced in *eve* mutant dMNs (Figures 2B, 2C, 2E, 2F, 2H, 2I, 2K, and 2L). Protein expression for Fas2 and Nrg is also reduced (Figure S3). Our results indicate that *eve* regulates mRNA levels of *Fas2*, *beat Ia*, *nrg*, and *unc-5* in aCC and RP2 and suggest that *eve* may program the guidance decisions of aCC and RP2 through the regulation of these cell surface molecules.

zfh1 and *grn* Regulate the Expression of Overlapping Subsets of *eve*-Regulated Cell Membrane Molecules

Previous studies have shown the involvement of two other transcriptional regulators of aCC and RP2 guidance, Zfh1, a Zn finger homeodomain family member, and Grain (Grn), a GATA family TF. While *zfh1* is expressed in all motoneurons including dMNs in the ISN nerve (Layden et al., 2006), *grn* expression in motoneurons is restricted to dMNs (Garces and Thor, 2006). Both can be regulated by *eve* or work in parallel to direct axon guidance (Garces and Thor, 2006). Furthermore, we have previously shown that *grn* can collaborate with *eve* to regulate *unc-5* (Zarin et al., 2012). Therefore, we investigated their requirement for *Fas2*, *beat Ia*, *nrg*, and *unc-5* expression in dMNs (Figures 2M–2X) and found that, while *Fas2*, *beat-Ia*, and *unc-5* are downregulated in aCC and RP2 neurons lacking *zfh1* (Figures 2M–2U), *nrg*'s mRNA is unaffected (data not shown). In *grn* mutants, only *unc-5* expression is reduced (Figures 2V–2X and data not shown). Together, these data indicate that *zfh1* and *grn* are required to selectively control overlapping subsets of *eve*-regulated genes and that *zfh1* is required for the regulation of a broader range of guidance molecules than *grn*.

ISN Guidance Requires the Combined Action of Attraction, Repulsion, and Adhesion

In *eve* mutants, the ISN almost never reaches its appropriate dorsal target muscles (Fujioka et al., 2003; Landgraf et al., 1999), whereas *beat Ia*, *nrg*, and *unc-5* single mutants only show partially penetrant defects in ISN projections (Fambrough and Goodman, 1996; Hall and Bieber, 1997; Labrador et al., 2005) (Figure 3). We reasoned that, since the expression of these genes is substantially decreased or absent in *eve* mutant motoneurons (Figure 2), their concerted function may be required for proper ISN guidance. To test this hypothesis, we analyzed

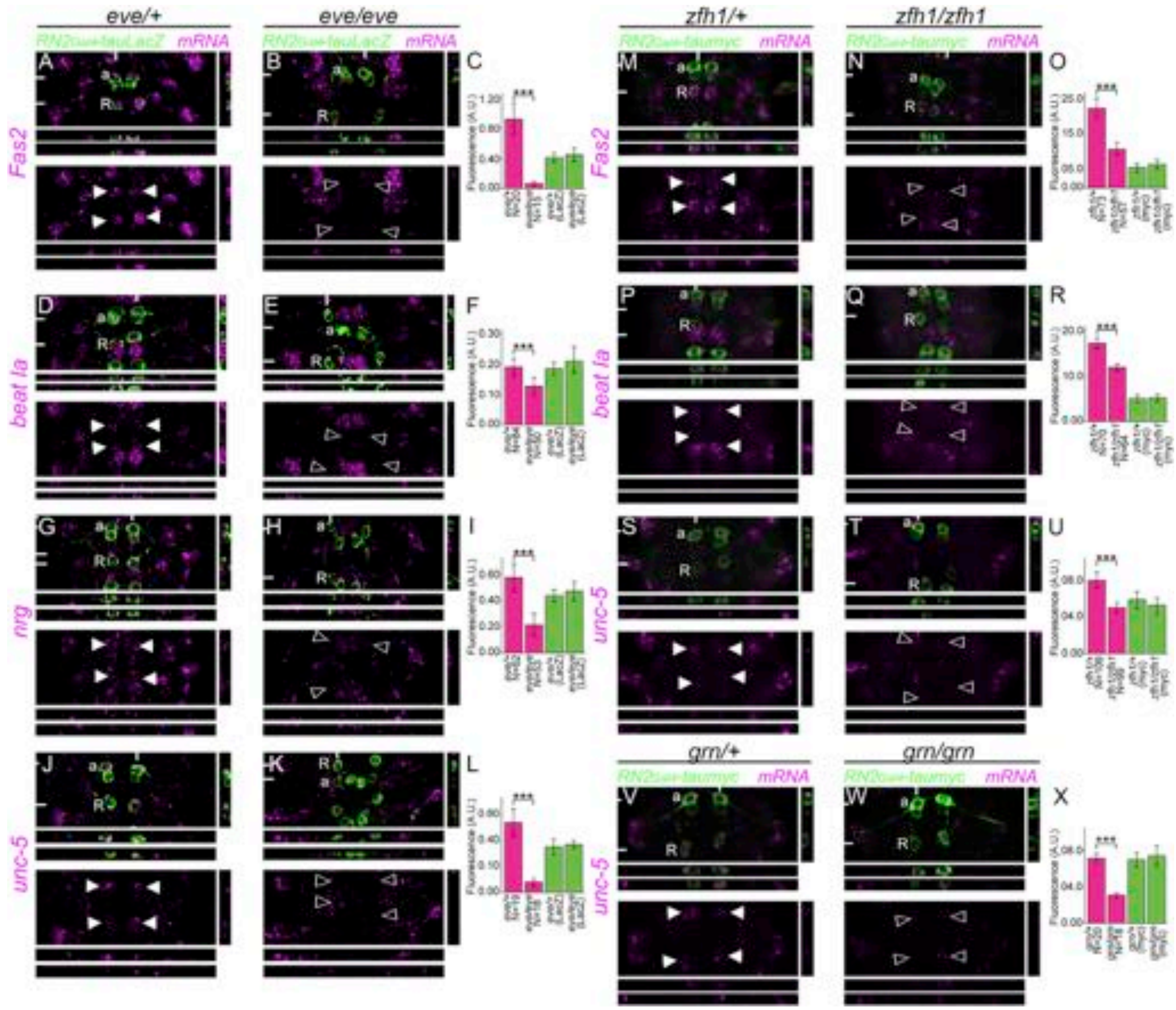

Figure 2. Regulation of *beat Ia*, *unc-5*, *nrg*, and *Fas2* in aCC and RP2 Motoneurons by *eve*, *zfh1*, and *grn*

The expression of *Fas2*, *beat Ia*, *nrg*, and *unc-5* mRNA was examined in aCC and RP2 (empty arrowheads) motor neurons of stage 15 *eve* mosaic embryos (B, E, H, and K) and their heterozygous siblings (arrowheads; A, D, G, and J), *zfh1* mutant embryos (empty arrowheads; N, Q, and T) and their heterozygous siblings (arrowheads; M, P, and S), and *grn* mutant embryos (empty arrowheads; V) and their heterozygous siblings (arrowheads; W) using in situ hybridization and confocal imaging. An *RN2-Gal4* driver is used to express *taumyc* and identify the aCC and RP2 motoneurons (green) and in situ signals (magenta). XZ and YZ sections are displayed below and to the right of each panel. In heterozygous embryos, clear expression of *Fas2* mRNA (A and M), *beat Ia* mRNA (D and P), *nrg* mRNA (G), and *unc-5* mRNA (J, S, and V) in both aCC and RP2 is observed. In *eve* mutant motor neurons, expression of these genes is substantially decreased in *Fas2* (B), *beat Ia* (E), *nrg* (H), and *unc-5* (K). In *zfh1* mutants, expression of *Fas2* (N), *beat Ia* (Q), and *unc-5* (T) is substantially decreased and in *grn* mutants only *unc-5* mRNA levels decrease (W). Graphs show the quantification of mRNA expression in aCC and RP2 neurons of heterozygous or mutant animals for each genotype for *Fas2* (C and O), *beat Ia* (F and R), *nrg* (I), and *unc-5* (L, U, and X). Genotypes and numbers of cells used in quantification are indicated on the x axis and fluorescence intensity as arbitrary units [a.u.] is indicated on the y axis. While there is no significant difference in expression level of Myc between heterozygous and mutant backgrounds, expression of all the genes shows statistically significant downregulation in aCC and RP2 neurons in mutant backgrounds. Data are represented as mean ± SEM. ***$p < 0.005$.

motor axon guidance phenotypes in double and triple mutants. The observed phenotypes are organized in order of severity, taking as a reference three branch points in the ISN from ventral to dorsal: first branch point (FB), second branch point (SB), and third branch point (TB), respectively (Figure 3A). Phenotypes present after TB are late phenotypes, between SB and TB intermediate phenotypes, and before FB the most severe early phenotypes (Figures 3N, 3O, and 3P, respectively). Double mutants display phenotypes not previously observed in single mutants (Table S2); for example, *nrg; unc-5* double mutants (Figure 3G) show aberrant crossings to the adjacent segment before the FB point (Figures 3C–3F). Additionally, the number of late defects is also substantially increased (double mutants 18% ± 0.02494%, *nrg* 4.3% ± 0.01381%, and *unc-5* 6.6% ± 0.01436%, respectively). Similarly, double mutants for *nrg* and *beat Ia* (Figure 3H) or *unc-5* and *beat Ia* (Figures 3I and 3J) exhibit stalling before FB (9% ± 0.03149% and 21% ± 0.02846%, respectively) only occasionally observed in *beat Ia* mutants (3% ± 0.01086%) (Figures 3E and 3F). Consistently, triple mutants present more severe phenotypes than double mutants (Figures 3K and 3L); in particular, ISN crossing in the ventral muscle field (from 2% ± 0.020%, 8.2% ± 0.029%, or 10% ± 0.044% in *nrg unc-5* double, *nrg*, *beat Ia* double, or *unc-5*, *beat Ia* double, respectively, to 15.3% ± 0.04382% in triple mutants; [Table S2]). In summary, single mutants generally present late phenotypes, while double mutant phenotypes are more severe and obvious in more ventral positions. The earliest, most severe, phenotypes are almost exclusively seen in double and triple mutants. ISN stall, in particular, is very similar to the defects observed in *eve* mosaic mutant embryos (Figure 3M). *eve* is still present in aCC and RP2 in these triple mutants, suggesting that neither these genes nor a target-derived BMP signal is required for *eve* expression (Aberle et al., 2002; Garces and Thor, 2006; Marqués et al., 2002) (Figure S4). Thus, dorsal targeting of the muscle field by the ISN is progressively affected by sequentially removing receptors and CAMs, suggesting the requirement of their combined action.

With the exception of Unc-5, these guidance molecules are not exclusively expressed in aCC and RP2 motoneurons within the ISN and their combined guidance defects also reflect their interactions with other axons within the same nerve at later stages of pathfinding. Therefore, some of the observed ISN phenotypes in compound mutants of guidance molecules are probably dependent on the loss of guidance molecules in the followers in addition to the pioneers such as early crosses as they are not observed in *eve* mutants. Therefore, we wanted to investigate the effect of mutations in these molecules at earlier stages of axon guidance, before aCC and RP2 leave the CNS, where they act as pioneers (Jacobs and Goodman, 1989; Sánchez-Soriano and Prokop, 2005). Given that Netrins are expressed in the midline (Harris et al., 1996; Mitchell et al., 1996) and Sidestep labels the path followed by aCC and RP2 (Siebert et al., 2009), we reasoned that combined mutations in their receptors may present exit phenotypes in these neurons as well. We used the *RN2-Gal4* driver to specifically label aCC and RP2 motor axons and examined their ability to exit the CNS in single and different mutant combinations (Figures 3Q–3V; Table S2). No single mutant presented any aCC or RP2 exit phenotype (Figure 3V; Table S2), consistent with the weak ISN guidance phenotypes of single mutants (Figures 3C–3F; Table S2). However, when both guidance receptors were eliminated, exit defects were observed (10% hemisegments [Figures 3S and 3T; Table S2]). Interestingly, embryos where either one of the receptors and the CAM Nrg were eliminated did not present any defect (Figures 3R and 3V; Table S2) and the elimination of *nrg* (or *Fas2*; data not shown) in the double receptor mutant did not significantly increase the observed exit defects. Unfortunately, we were unable to generate quadruple mutant animals to determine the effect of removing both CAMs. These results suggest that directed guidance toward the muscle field and away from the midline is an important driving force for aCC and RP2 exit and the combined action of Unc-5 and Beat Ia contributes to this process. Nevertheless, the strong phenotypes observed in *eve* mutants and relatively mild ones in double receptor mutants indicate that *eve* regulates pioneer exit through additional genes not analyzed in the present study.

eve Interacts Genetically with *nrg, beat Ia*, and *unc-5*

In order to dissect the functional link between *eve* and its downstream targets in dMN guidance, we examined genetic interactions between them. We have previously shown a transheterozygous interaction between *eve* and *unc-5*, suggesting that both genes work together during ISN guidance (Zarin et al., 2012). We used this transheterozygous combination as a sensitized background to further reduce *beat Ia* levels to 50% and identified significantly increased ISN defects (number of axons exhibiting stalls from 3.0% ± 0.010% to 7.5% ± 0.022% in $eve^{\Delta RP2}$/+, $unc\text{-}5^{8}$/+ transheterozygous and $eve^{\Delta RP2}$/+, $unc\text{-}5^{8}$/+, *beat* Ia^{3}/+ triple transheterozygous, respectively [Figures 4D and 4F; Table S2] or from 8.1% ± 0.020% to 23.1% ± 0.036%, when eve^{3} and *beat-Ia* ^{C163} null alleles were used [Figure 4G; Table S2]). We next compared ISN defects in *nrg*/*Y* hemizygote mutants with *nrg*/*Y; eve*/+ animals. Removing one copy of *eve* in *nrg* mutant embryos resulted in more severe ISN guidance defects with significant increases in stalls (from 3% ± 0.014% to 21.2% ± 0.038% in nrg^{3}/*Y* or nrg^{3}/*Y;* $eve^{\Delta RP2}$/+, respectively; similar effects, although somewhat weaker, were found when a hypomorphic nrg^{2} allele was used [Figures 4C and 4E; Table S2]). These results suggest that, in addition to *nrg*, *eve* regulates other genes that work in parallel to *nrg* as part of its guidance output.

Combinatorial Expression of Cell Surface Molecules Reveals Their Individual Function and Restores CNS Exit

In *eve* mutants, aCC and RP2 fail to exit the CNS and thus provide an ideal genetic background to determine the individual function of the identified guidance molecules in aCC and RP2 guidance. To test this idea, we expressed *unc-5*, *beat Ia*, *nrg*, and *Fas2* individually or in combination in *eve* mutant dMNs.

Expressing either of these cell surface molecules alone in *eve* mutants leads to exit of a single motoneuron of the pair per hemisegment (only when *unc-5* is re-expressed 11% ± 0.014% of hemisegments show dual exit [Figures 5B–5E and 5N; Table S3]). Axonal exit ranged from no further exit beyond what is seen in *eve* mutants with *nrg* (10% ± 0.036% of hemisegments with single motoneuron exit) to some increase of dorsal projections with *Fas2*, *beat Ia*, or *unc-5* (25% ± 0.024%, 36% ± 0.052%, and 67% ± 0.030% of hemisegments, respectively, with single motoneuron exit).

Expressing two of these surface molecules leads to a more robust exit where many hemisegments show exit of both motoneurons (Figures 5F–5J and 5N). The only exception is when both CAMs are re-expressed (26% ± 0.036% single motoneuron exit [Figure 5N; Table S3]). We observe two different types of dual exit: unfasciculated, both axons from the same hemisegment chose a different nerve root, or fasciculated,

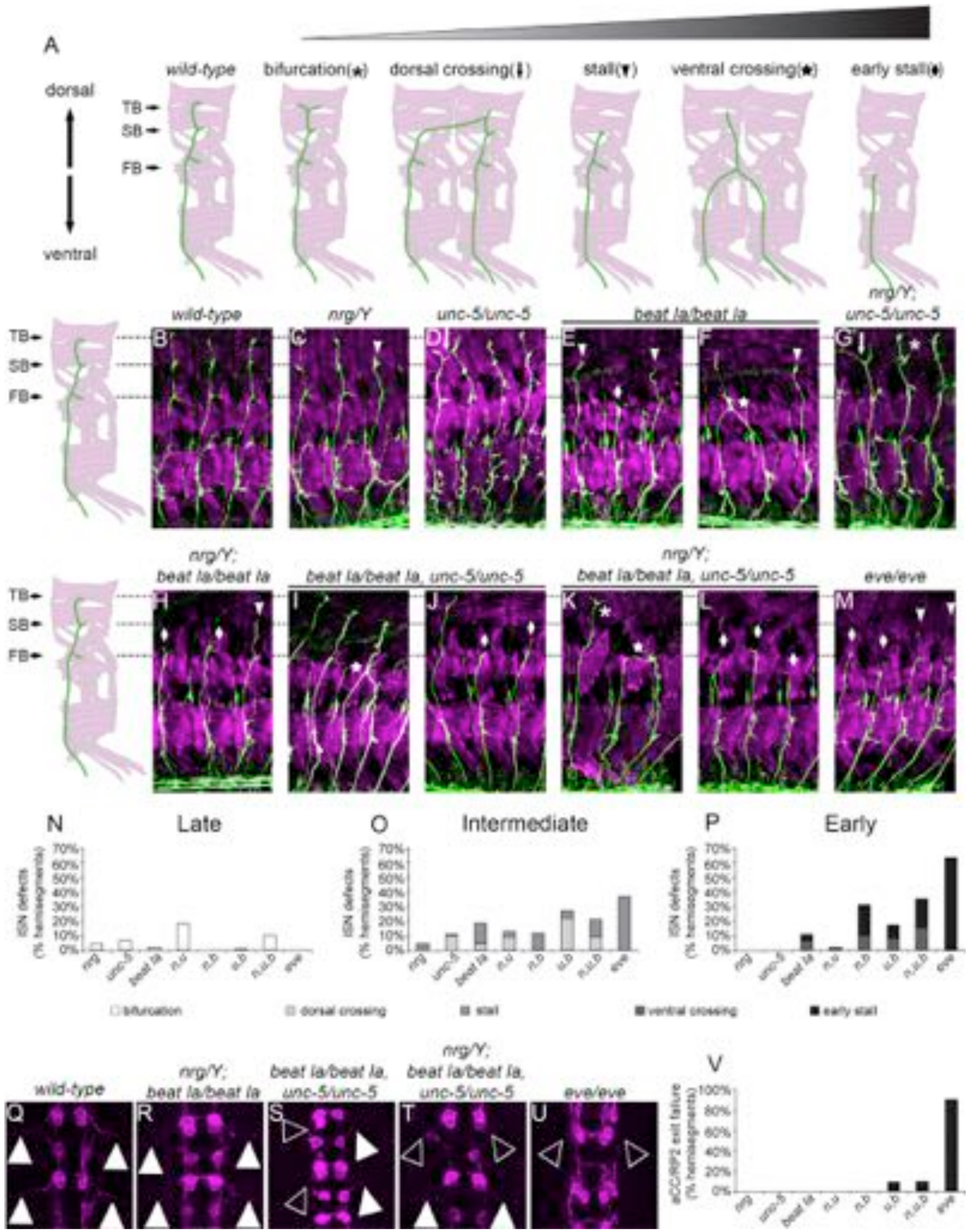

(legend on next page)

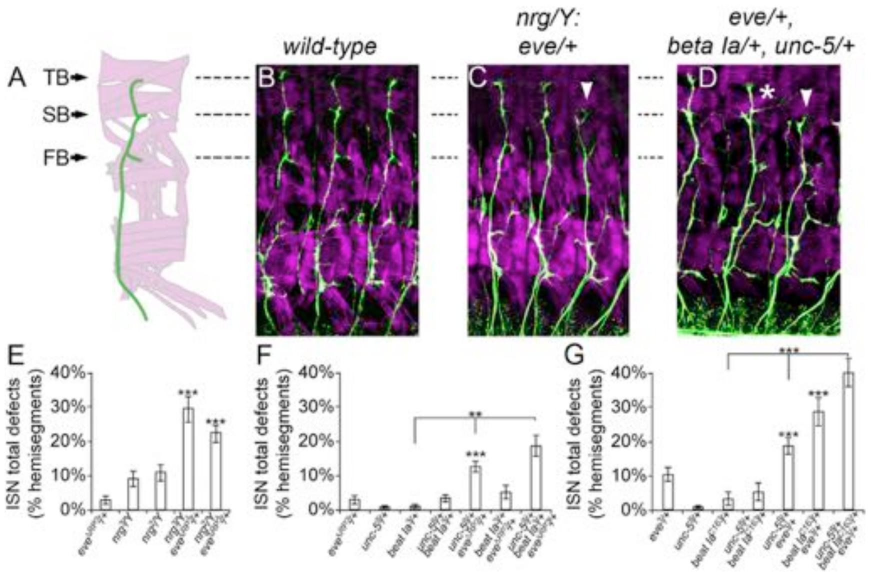

Figure 4. *eve* Interacts Genetically with *nrg*, *beat Ia*, and *unc-5*

(A) Schematic depiction of a single hemisegment in a wild-type late stage 16 embryo illustrating ISN motor axons (green) and body wall muscles (magenta). Black arrows point to the first (FB), second (SB), and third (TB) branching point of the ISN.

(B–D) Flat-mounted late stage 16 embryos stained with anti-Fas2 and anti-myosin antibody to visualize the motor axons (green) and muscles (magenta), respectively. Anterior is shown on the left and dorsal is shown on the top in all panels. Partial genotypes are indicated above each panel. In wild-type (B), ISN innervates dorsal muscles and respects segment boundaries. In *nrg/Y; eve/+* embryos (C) or *unc-5/+; beat Ia/+; eve/+* embryos (D), some ISNs stall before reaching their target muscles (white arrowhead) and some others cross the segment boundary (white star).

(E–G) Quantification of total ISN defects in embryos heterozygous for *eve*, hemizygous for *nrg*, or heterozygous for *eve* and hemizygous for *nrg* together (E). Quantification of total ISN defects in embryos heterozygous for $eve^{\Delta RP2}$, *beat* Ia^{3}, or $unc\text{-}5^{8}$ and their different transheterozygous combinations (F). Quantification of total ISN defects in embryos heterozygous for eve^{3}, *beat* Ia^{C163}, or $unc\text{-}5^{8}$ and their different transheterozygous combinations (G). Data are represented as mean ± SEM. $^{**}p < 0.05$, $^{***}p < 0.005$.

when axons join and exit through the ISN root (Figure 5O). Interestingly, there is a higher ratio of fasciculated to unfasciculated exit when combinations of a receptor and a CAM are re-expressed than when both receptors are expressed. These data, together with the failure of the combined expression of the two CAMs to promote dual exit, suggests that receptors promote directed guidance away from the midline (Figures 3S, 3T, and 3V) and CAMs are required for the fasciculation of the migrating axons. Finally, reintroducing combinations of three surface molecules results in the highest percentage of exit (85% ± 0.019% or 90% ± 0.029% when *unc-5*, *beat*, and *nrg* or *unc-5*, *beat*, and *Fas2* are reintroduced, respectively [Figures 5K, 5L, and 5N]). Most of the hemisegments show fasciculated exit (66% ± 0.014% fasciculated versus 12% ± 0.016% unfasciculated in *unc-5*, *beat*, and *nrg* or 70% ± 0.055% fasciculated versus 11% ± 0.034% unfasciculated in *unc-5*, *beat*, and *Fas2* [Figure 5O; Table S3]) and fasciculated axons exit through the ISN root. Nevertheless, the strong effect on exit of their combined re-expression strikingly contrasts with the relatively mild effect of their combined loss of function (Figures 3Q–3V; Table S2), indicating that, while these gain-of-function experiments reveal the function of individual genes or their combinations through re-expression/overexpression, they do not necessarily reveal the extent of their endogenous contribution. Together, these findings suggest that the concerted expression and coordinated function of guidance receptors and CAMs can induce the proper exit from the CNS and fasciculation of motor axons.

Figure 3. The Coordinated Function of Attractive, Repulsive, and Adhesive Molecules Is Required for ISN Axon Guidance

(A) Schematic depictions of wild-type and different mutant phenotypes in late stage 16 embryos illustrating ISN motor axons (green) and body wall muscles (magenta). Black arrows point to the first (FB), second (SB), and third (TB) branch points of the ISN. The severity of phenotypes increases from left to right and different symbols for each phenotype observed are to the right of their description.

(B–M) Flat-mounted late stage 16 embryos stained with anti-Fas2 and anti-myosin antibody to visualize the motor axons (green) and muscles (magenta), respectively. Anterior is shown on the left and dorsal is shown on the top in all panels. Partial genotypes are indicated above each panel. (B) In wild-type, ISN innervates dorsal muscles and respects segment boundaries. (C) *nrg/Y* mutant embryo where one ISN stalls before reaching the dorsal muscles. (D) Embryos lacking *unc-5* show ISN dorsal crossing. (E and F) *beat Ia* mutant embryos showing ISN stall, ISN ventral crossing, and ISN early stall. (G) *nrg; unc-5* double mutants showing ISN bifurcations and ISN dorsal crossing. (H) *nrg; beat Ia* double mutant embryo in which two ISNs stall very early and one ISN stalls before the reaching the most dorsal muscles. (I and J) *beat Ia, unc-5* double mutants displaying early ISN ventral crossing and early ISN stalls. (K and L) *nrg; beat Ia, unc-5* compound mutants present ISN bifurcation, ISN ventral crossing, and ISN early stalls. (M) ISNs in *eve* mosaic embryos lacking *eve* in aCC and RP2 motor neurons show both early and late stalls.

(N–P) Quantification of ISN defects in different genetic backgrounds. The phenotypes were divided into three categories: ISN bifurcation as late phenotypes (mild in severity) (N), ISN tip loss and ISN dorsal cross as intermediate phenotypes (moderate in severity) (O), and ISN early stall and ISN ventral cross as early phenotypes (most severe) (P). An *RN2-Gal4* driver is used to express *taumyc* and visualize the axonal projections of aCC and RP2 motor neurons in flat-mounted stage 13 embryos (Q–V).

(Q) Motor axons of wild-type *aCC* and *RP2* neurons fasciculate with each other and exit the CNS (arrowheads).

(R–T) Lateral projection of *aCC* and *RP2* motor axons in *nrg;beat Ia* double mutants is normal (R). *aCC* and *RP2* motor axons fail to exit the CNS in 10% of hemisegments in *beat Ia, unc-5* (S) or *nrg; beat Ia, unc-5* (empty arrowheads) (T) compound mutants.

(U) In *eve* mutant aCC and RP2 motor neurons, the majority of these motor axons (91%) fail to exit the CNS (empty arrowheads).

(V) Quantification of CNS exit failure in different genetic backgrounds (*n*, *nrg*; *u*, *unc5*; *b*, *beat Ia*).

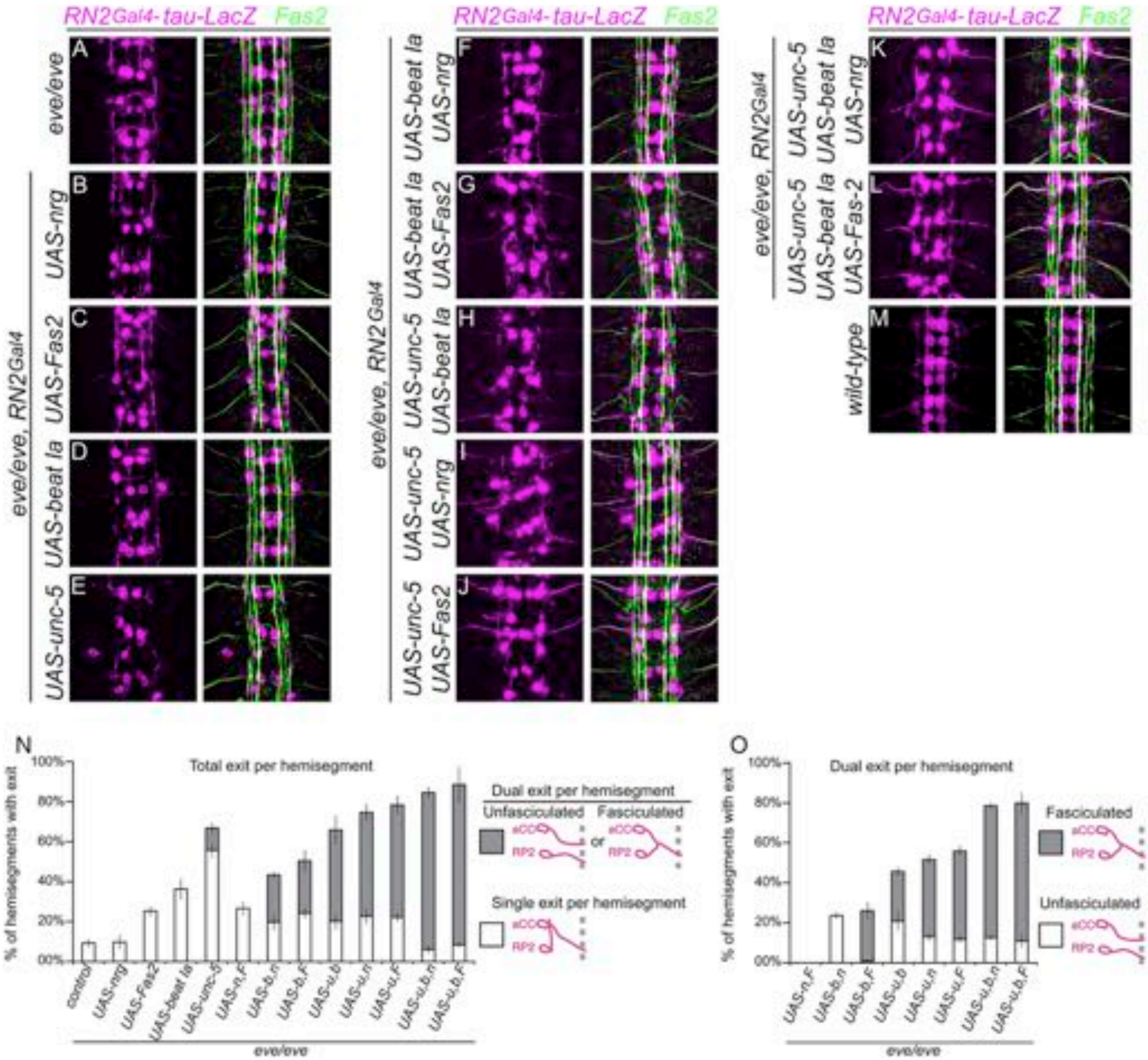

Figure 5. Combined Expression of Cell Surface Molecules Partially Restores CNS Exit

Axonal projections of aCC and RP2 visualized with an *RN2-Gal4* driver expressing *UAS-tau-LacZ* (magenta) in flat-mounted stage 16 embryos. To better localize and trace the motor nerve exit of these motoneurons, embryos were also stained with anti-Fas2 antibody (green). Anterior is shown on top in all panels and partial genotypes are indicated on the left of each panel.

(A) aCC and RP2 axons in over 90% of hemisegments in *eve* mosaic embryos fail to exit the CNS and some of these axons cross the midline; a phenotype that is absent in wild-type aCC and RP2 neurons (M).

(B–E) Individual re-expression in *eve* mutant aCC and RP2 motoneurons of *UAS-nrg* (B), *UAS-Fas2* (C), *UAS-beat Ia* (D), or *UAS-unc-5* (E).

(F–J) Simultaneous re-expression of two membrane molecules: *UAS-beat Ia* and *UAS-nrg* (F), *UAS-beat Ia* and *UAS-Fas2* (G), *UAS-beat Ia* and *UAS-unc-5* (H), *UAS-nrg* and *UAS-unc-5* (I), or *UAS-Fas2* and *UAS-unc-5* (J).

(K and L) Combinatorial re-expression of *UAS-unc-5*, *UAS-beat Ia*, and *UAS-nrg* (K) or *UAS-unc-5*, *UAS-beat Ia*, and *UAS-Fas2* (L) in *eve* mutant aCC and RP2 restore exit and fasciculation in 66% and 69% of hemisegments, respectively.

(N) Quantification of total exit for aCC and RP2 in different genetic backgrounds divided between dual exit (either fasciculated or not) of both motoneurons and single exit of either one of them per hemisegment. Single re-expression of any individual gene leads to almost exclusively single exit. Single or dual re-expression of both CAMs (Nrg of Fas2) leads only to single exit in 26% of the hemisegments.

(O) Quantification of dual exit in different backgrounds in which two or more genes are reintroduced in *eve* mutant aCC and RP2. Dual exit is divided between fasciculated or nonfasciculated exit. The ratio of fasciculated to unfasciculated exit increases when a CAM is re-expressed with one or both guidance receptors (*unc-5* or *beat Ia*). From 25%/21% fasciculated/unfasciculated when *unc-5* and *beat Ia* are reintroduced to 66%/13% or 69%/11% fasciculated/unfasciculated when both receptors are reintroduced with *nrg* or *Fas2*, respectively. Data are represented as mean ± SEM.

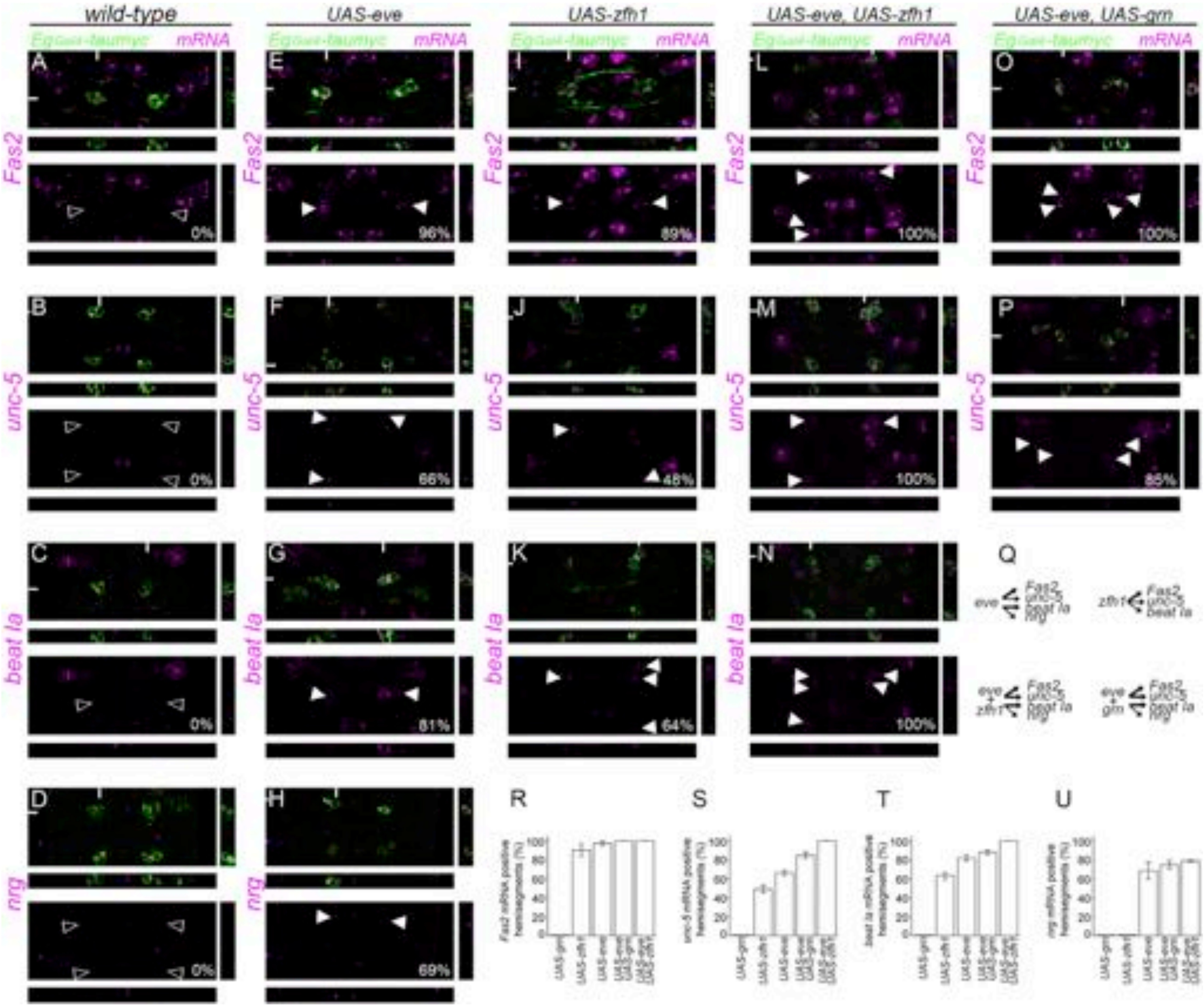

Figure 6. Misexpression of *eve* in EW Interneurons Is Sufficient to Induce the Repertoire of Cell Surface Molecules of aCC and RP2 but Combined Misexpression of *eve* with *zfh1* or *grn* Induces a More Robust Response

The mRNA expression of *Fas2*, *nrg*, *beat Ia*, and *unc-5* was examined in EW neurons of stage 16 embryos using in situ hybridization and confocal imaging (in magenta). To identify EW cells, we used an eagleGal4 driver to express UAS-tau-myc (green; arrowheads or empty arrowheads). XZ and YZ sections are displayed below and at the right of each panel, respectively. The percentage of hemisegments expressing mRNA for each gene is shown on the bottom left of each panel.

(A–D) There is no evidence for expression of *Fas2* (A), *unc-5* (B), *beat Ia* (C), or *nrg* (D) mRNA in wild-type EW neurons (empty arrowheads).

(E–H) ectopic expression of *UAS-eve* in EW induces their expression in these cells (arrowheads) *Fas2* (E), *unc-5* (F), *beat Ia* (G), and *nrg* (H).

(I–K) Individual misexpression of *UAS-zfh1* results in induction of *Fas2* (I), *unc-5* (J), and *beat Ia* (K) expression.

(L–M) Combined misexpression of *eve* with *zfh1* leads to strong expression of *Fas2* (L), *unc-5* (M), and *beat Ia* (N) in 100% of hemisegments.

(O and P) Combined misexpression of *eve* with *grn* leads to strong expression of *Fas2* (O) and *unc-5* (P).

(Q) Schematic illustration of the transcriptional regulation of *Fas2*, *unc-5*, *beat Ia*, and *nrg* by different transcription factors and combinations; the thickness of the arrow represents the strength of induction.

(R–U) Graphical representation of the induction of *Fas2* (R), *unc-5* (S), *beat Ia* (T), and *nrg* (U) by the different transcription factors or combinations. Data are represented as mean ± SEM.

Ectopic Expression of *eve* in Interneurons Induces the Expression of Cell Surface Molecules of dMNs

Our previous data show that *eve* is required for the coordinated expression of an array of cell surface molecules in aCC and RP2 motoneurons (Figure 2). To determine whether *eve* is sufficient to induce their expression in other neurons, we identified a group of *eagle* interneurons that do not express *eve* or any of those four surface molecules, the EW neurons, which project axons across the posterior commissure (Higashijima et al., 1996) (Figures 6A–6D). We used the *eagleGAL4* driver (Dittrich et al., 1997) to

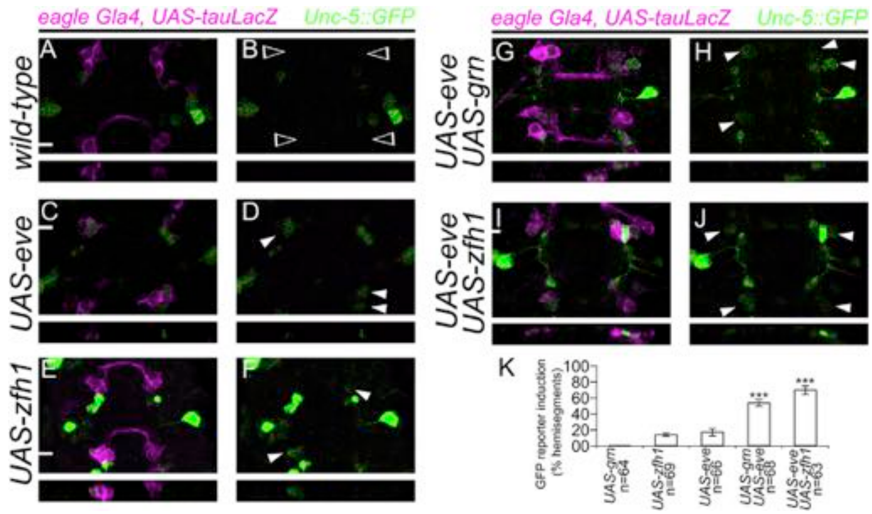

Figure 7. A *unc-5* Neuronal Enhancer Is Combinatorially Regulated by *eve* and *zfh1* or eve and *grn*

(A–J) A *unc-5* neuronal enhancer that drives expression of GFP (unc5::NLS-GFP) in motoneurons was used to examine its regulation by combinations of transcription factors in EW neurons of stage 16 embryos using immunostaining and confocal imaging. To identify EW cells, we used an eagleGal4 driver to express UAS-tau-lacZ (left). There is no evidence for expression of GFP in wild-type EW neurons (empty arrowheads; A and B). However, misexpression of *UAS-eve* (C and D) or *UAS-zfh1* (E and F) is able to drive GFP expression from the *unc-5* reporter (arrowheads). Combinatorial expression of *UAS-eve* and *UAS-grn* (G and H) or *UAS-eve* and *UAS-zfh1* (I and J) induces a much more robust expression of GFP than *UAS-eve* or *UAS-zfh1* alone (arrowheads).

(K) Graphical representation of the reporter activation when a single or combinations of transcription factors are misexpressed in EW neurons. Data are represented as mean ± SEM. ***$p < 0.005$.

misexpress *eve* in EW neurons and analyzed the induction of *Fas2*, *unc-5*, *beat Ia*, and *nrg* by in situ hybridization. While none of these genes' mRNA was expressed in wild-type EW neurons (Figures 6A–6D), ectopic expression of *eve* resulted in their transcriptional induction (*Fas2* in 96%, *unc-5* in 66%, *beat Ia* in 81%, and *nrg* in 69% of the scored hemisegments [Figures 6E–6H and 6R–6U]). Additionally, Fas2 and Nrg protein expression is absent in wild-type EWs (Figures S5A, S5B, S5E, and S5F) but *eve* misexpression led to their ectopic induction (Figures S5C, S5D, S5G, and S5H). These results show that *eve* is sufficient to transcriptionally reprogram EW interneurons to express the same array of molecules it regulates in dorsal motoneurons.

Combined Misexpression of *eve* with *grn* or *zfh1* Induces Robust Expression of Cell Surface Molecules from dMNs in Interneurons

Since *zfh1* and *grn* are partially required for the transcriptional regulation of a subset of *eve* downstream genes in aCC and RP2 neurons (Figures 2M–2X), we tested whether they were also sufficient to induce them in EWs. Similar to *eve*, neither *grn* nor *zfh1* are expressed in these interneurons (Figures S6A, S6B, S6E, and S6F). Individual misexpression of *zfh1* in EWs induces *Fas2*, *beat-Ia*, and *unc-5* expression in 89%, 64%, and 48% of scored hemisegments, respectively (Figures 6I–6K and 6R–6U); however, *grn* alone is not sufficient to induce expression of any of these genes (Figures 6R–6U). Given their partial requirement for the induction of some of these genes (Figures 2M–2X), we hypothesized that coexpression of *eve* with either *grn* or *zfh1* may elicit a more robust transcriptional response. Indeed, combined misexpression of *eve* with *zfh1* robustly induced *Fas2* in 100% of the segments in EWs, with a much stronger signal than *eve* alone (fluorescence intensity 10.9 ± 1.7 a.u. and 19.3 ± 1.1 a.u. for *eve* alone and *eve*, *zfh1* dual misexpression, respectively; $p < 0.005$), as well as *unc-5* and *beat-Ia* (Figures 6L–6N and 6R–6T) but not *nrg* (Figure 6U). In addition, misexpression of *eve* and *grn* together lead to a significant increase of EWs expressing *Fas2* (fluorescence intensity 18.4 ± 1.4 a.u.; $p < 0.005$) and *unc-5* (100% and 85% hemisegments, respectively [Figures 6O, 6P, 6R, and 6S]) but not a significant increase in *beat Ia* or *nrg* expression beyond *eve* induction alone (Figures 6T and 6U). Importantly, *eve* does not induce *zfh1* or *grn* in EWs (Figure S6), indicating that they work in parallel to *eve* in EWs to promote transcription of these receptors and CAMs.

These data suggest that *zfh1* is sufficient to promote transcription of some of the dMN guidance molecules in EWs but *grn* is not. However, both *zfh1* and *grn* can work together with *eve* to transcriptionally reprogram EWs and regulate guidance receptors and CAMs normally expressed in dMNs. Additionally, the combinatorial expression of *eve* with *zfh1* or *grn* induces a more robust transcriptional reprograming of EWs than each of them alone (Figure 6Q).

The *unc-5* Neuronal Enhancer Is Combinatorially Regulated In Vivo by *eve*, *zfh1*, and *grn*

To understand how these regulators work together in vivo to regulate gene expression, we took advantage of the previously characterized *eve*-dependent *unc-5* neuronal enhancer that drives expression in aCC and RP2 dMNs (Zarin et al., 2012). We used this enhancer to generate a GFP reporter that is expressed in aCC and RP2 under the control of *eve* (Figure S7) and tested whether *eve* is sufficient to regulate the reporter in EW neurons independently of *zfh1* and *grn*. The *unc-5* reporter is not expressed in EWs (Figures 7A and 7B). In contrast, *eve* misexpression in EWs leads to GFP reporter activation (17% of hemisegments [Figures 7C, 7D, and 7K]). These results indicate that *eve* is able to regulate transcription through the *unc-5* neuronal enhancer independently of *zfh1* and *grn*. In order to determine whether *zfh1* or *grn* were also sufficient to regulate this enhancer, we misexpressed them in EWs. Only *zfh1* was able to induce the GFP reporter expression through this enhancer element (14% of hemisegments [Figures 7E, 7F, and 7K]). As *eve* can work together with *grn* and *zfh1* to induce *unc-5* expression in EWs (Figures 6M and 6P), we reasoned that this regulatory region might be able to integrate the effect of combinations of these TFs. Hence, we misexpressed *eve* and *grn* (Figures 7G and 7H) or *eve* and *zfh1* combinations in EWs in the presence of the reporter (Figures 7I and 7J). Combined expression of either *zfh1* or *grn* with *eve* led to a substantial induction of the reporter in EWs (53% and 68% of the hemisegments when *eve* is combined with *grn* or *zfh1*, respectively [Figure 7K]), indicating that *eve* and *grain* or *zfh1* can act synergistically to induce *unc-5* through the same regulatory region. As *grn* and *zfh1* are not induced by *eve* in EW neurons, this cooperative activation requires the individual presence of each of these TFs. Together, these data indicate that *eve* and *zfh-1* are sufficient to regulate transcription in vivo through the *unc-5* neuronal enhancer element. Additionally, *grn* and *zfh1* can collaborate with *eve* to induce a more robust transcriptional response through the same regulatory region that regulates *unc-5* expression in aCC and RP2 dMNs.

Misexpression of *eve* or Combined Misexpression of Its Downstream Cell Surface Molecules Can Reprogram the Guidance Behavior of Interneurons

We next wanted to test whether expression of *eve* in EW neurons would also alter their guidance behavior. Indeed the axons of EW neurons that express *eve* no longer cross the CNS midline remaining ipsilateral and some project toward the muscle field (24% ± 0.029%) (Figures 8H and 8N). We reasoned that if the surface molecules that *eve* regulates in them mediate the guidance switch it promotes in EW interneurons, we might be able to reprogram their guidance by ectopically expressing these molecules. To test this idea, we used *eagleGAL4* to misexpress each of these four genes alone or in different combinations and traced their axons (Figures 8B–8F). Individual genes did not lead to EW projections into the muscle field except for a small number when *unc-5* was misexpressed (3% ± 0.012% hemisegments [Figures 8C and 8G]). Expression of *unc-5*, however, prevented EW axons from crossing the midline, similar to *eve* misexpression (Figure 8H). Expression of double, triple, and quadruple combinations of membrane molecules had an increasing effect on CNS exit (Figures 8D–8G). Interestingly, a combination of both CAMs (*nrg* and *Fas2*) had no effect on exit but each one individually or in combination had an enhancing effect in the presence of *unc-5* or both guidance receptors (from 5% ± 0.019% exit when *beat Ia* and *unc-5* are combined to 20% ± 0.041% when *nrg* is also present and up to 33% ± 0.049% if the four are misexpressed [Figures 8D and 8G]). Moreover, EW axon rerouting by *eve* is significantly suppressed (to 14% ± 0.013%) and midline crossing is also partially restored when *eve* is missexpressed in a *beat Ia* and *unc-5* double mutant background (Figures 8I and 8N). To determine the effect of these molecules on guidance in the muscle field, we also misexpressed them in ventral MNs (vMNs). *eve* misexpression in vMNs leads to dorsalization of the ISNb branch, where it overshoots ventral muscles and projects into the dorsal muscle field (Landgraf et al., 1999). Since *eve* regulates all of these guidance molecules, we would predict that their combined misexpression would lead to a stronger rerouting of vMNs. Indeed, combined misexpression leads to an increasingly stronger dorsal projection when both receptors or both receptors and CAMs are expressed (Figure S8).

Our data demonstrate that the combinatorial expression of *unc-5*, *beat Ia*, *nrg*, and *Fas2* can redirect EW axons to join the motor axon roots and exit toward the muscle field as motoneurons do. *eve* can not only reprogram EW interneurons to express these genes but can also alter their guidance decisions to resemble dMNs. Furthermore, this reprogramming of axonal projections is dependent on the molecules it normally regulates in aCC and RP2.

Combined Misexpression of *eve* with *zfh1* or *grn* Leads to a Stronger Reprogramming of the Guidance Behavior of Interneurons

Considering the robust expression of guidance molecules by a combinatorial expression of *eve* and *zfh1* or *grn* (Figures 6 and 7), our prediction was that their combined misexpression would also lead to a more significant axonal exit from the midline. Consistent with its ability to induce expression of different *eve* downstream targets (Figures 6I–6K), ectopic expression of *zfh1* induced EW exit in 24% ± 0.065% of the hemisegments. Within a given segment, some EW axons still crossed the midline and others projected laterally (Figures 8K and 8N), as previously reported (Layden et al., 2006). In line with its inability to induce expression in EWs, *grn* alone did not change their projection patterns (Figures 8J and 8N). However, combined ectopic expression of *eve* with either *grn* or *zfh1* led to a strong lateral exit of EW axons in 72% ± 0.058% and 80% ± 0.050% of hemisegments, respectively (Figures 7L, 7M, and 7N).

Consistent with their combined effect on the expression of receptors and CAMs, coexpression of *eve* with *grn* or *zfh1* redirects EW axons more robustly than when *eve* is misexpressed alone. These results highlight the combinatorial requirement of membrane guidance molecules as well as the combined action of *eve* with *zfh1* and *grn* for efficient reprogramming of EW's axonal projections.

DISCUSSION

Microarray analysis and single-cell resolution expression data have allowed us to establish how *eve*, a motoneuron subclass determinant, regulates axonal trajectories partially through the coordinated regulation of a series of membrane receptors and CAMs. We also show that this repertoire of molecules functions in individual dorsal pioneer motoneurons to orchestrate adhesive, repulsive, and attractive forces that can work together to steer their axons in the correct path and pioneer the ISN nerve branch. Furthermore, we also show that two other transcriptional regulators expressed in aCC and RP2 dMNs, *grn* and *zfh1*, can work in parallel and in cooperation with *eve* to regulate the expression of subsets of these molecules.

Regulation of a Full Program of Axon Guidance in Dorsal Motoneurons

The connection between TFs and the guidance genes that they regulate has been generally elusive. Transcriptional regulators with tissue or cell-specific expression patterns may control local expression of multiple pathfinding genes, frequently broadly

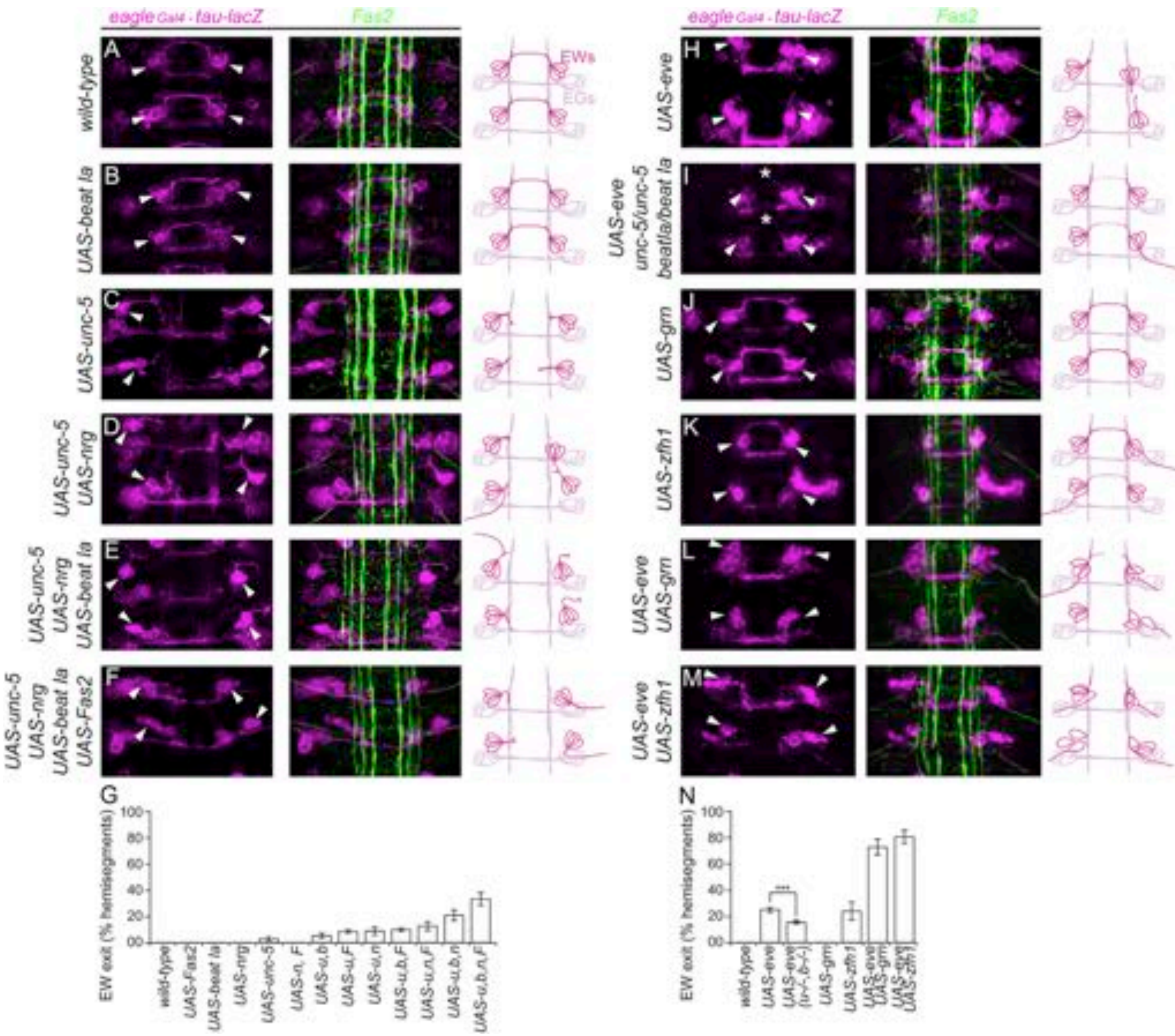

Figure 8. Misexpression of *eve* or the Combined Misexpression of Its Downstream Cell Surface Molecules Can Reprogram the Guidance Behavior of EW Interneurons

An *eagle-Gal4* driver is used to express *tau-LacZ* and visualize the axonal projections of EW interneurons in flat mounted stage 16 embryos (magenta). To better localize and trace the EW axons, we also stained embryos with anti-Fas2 antibody (green). Partial genotypes are indicated to the left of each panel and a cartoon representing EW projections to the right.

(A) Axons of wild-type EW neurons fasciculate and project across the posterior commissure.

(B) No significant difference is observed in axonal projection of EW neurons misexpressing *UAS-beat Ia*.

(C) EW neurons misexpressing *UAS-unc-5* do not cross the midline but fail to project laterally.

(D) Combinatorial misexpression of *UAS-unc-5* with *UAS-nrg* results in lateral exit of 8% of EW axons.

(E and F) Triple misexpression of *UAS-unc-5*, *UAS-beat Ia*, and *UAS-nrg* (E) or quadruple misexpression of *UAS-unc-5*, *UAS-beat Ia*, *UAS-nrg*, and *UAS-Fas2* (F) in EW neurons leads to lateral redirection of axons in 20% or 33% of hemisegments, respectively.

(G) Quantification of lateral projection of EW axons in different genetic backgrounds. *F*, *Fas2*; *n*, *nrg*; *b*, *beat Ia*; *u*, *unc-5*.

(H–N) The combined misexpression of *eve* with *grn* or *zfh1* leads to a stronger lateral exit of EW axons than *eve* alone. (H) In almost all of EW neurons, misexpressing *UAS-eve* axons fail to cross the midline and in 25% of hemisegments project laterally and join the motor roots. (I) CNS exit from EW neurons misexpressing *UAS-eve* is partially suppressed in the absence of *unc-5* and *beat Ia* (15%), and midline crossing is partially restored (white asterisks). (J) Individual misexpression of *grn* has no effect on EW guidance behavior. (K) Misexpression of *UAS-zfh1* leads to EW exit (24% of hemisegments) and thinning of the commisural projections. (L and M) Combinatorial misexpression of *eve* with *grn* (L) and *eve* with *zfh1* (M) induces strong exit of EW axons in 72% and 80% of hemisegments, respectively. (N) Quantification of lateral projection of EW axons in different genetic backgrounds. Data are represented as mean ± SEM. $^{***}p < 0.005$.

expressed and whose individual elimination leads in general to mild phenotypes. In our study, we provide several lines of evidence to demonstrate that *eve* partially controls guidance of dorsal motoneuron axons through the regulation of at least two guidance receptors (Unc-5 and Beat-Ia) and two CAMs (Nrg and Fas2), highlighting the requirement of multiple guidance systems downstream of *eve*.

Similarly, in several well-established systems, individual TFs play a critical role in axon guidance. For example, during dorsal motor axon growth in the limb, the Lim1/Lhx1, a lim family TF, is exclusively expressed in the lateral set of neurons within the lateral motor column (LMC(l)) that projects to the dorsal side of the limb mesenchyme. Its absence renders LMC(l) motoneurons unable to distinguish between dorsal and ventral limb (Kania et al., 2000). Lhx1 regulates EphA4 in LMC(l) and misexpression of EphA4 can redirect ventral axons dorsally (Kania and Jessell, 2003). Nevertheless, other guidance cues have been identified that together with EphA4 control dorsal steering of LMC(l) motor axons such as Ret and ephrinAs (Bonanomi et al., 2012; Dudanova et al., 2010, 2012; Kramer et al., 2006). However, whether Lhx1 also controls these other pathways is unknown.

How Does *eve* Regulate Dorsal Motoneuron Guidance Receptors?

Eve has a dual role in motoneuron guidance. First, it blocks the expression of the ventral motoneuron-specific TFs HB9, Nkx6, and Lim3 (Broihier et al., 2004; Broihier and Skeath, 2002; Fujioka et al., 2003; Odden et al., 2002), which in turn regulate ventral-specific adhesion molecules such as Fas3 (Broihier et al., 2004). Second, *eve* can regulate the expression of two other TFs, Grn and Zfh1 (Garces and Thor, 2006), responsible for the expression of guidance genes in dMNs such as *unc-5* (Zarin et al., 2012). In *grn* (Garces and Thor, 2006) or *zfh1* (Layden et al., 2006) mutants, the ISN fails to reach its dorsal muscle targets, although their phenotype is less severe than that of *eve* alone, suggesting that each one might be responsible for only part of *eve*'s guidance output (Garces and Thor, 2006; Layden et al., 2006). Our results suggest that this is the case as mRNA levels of only subsets of *eve*-regulated guidance receptors and CAMs are controlled by *grn* or *zfh1* in dMNs (Figure 2).

While *zfh1* and *grn* are the only identified effectors regulating guidance downstream of *eve*, they also work in parallel in a cell-dependent manner (Garces and Thor, 2006; Zarin et al., 2012). We show that *eve* is able to induce expression of *Fas2*, *beatIa*, *unc-5*, and *nrg* in a *grn*- and *zfh1*-independent manner, indicating that *eve* can also work at the same hierarchical level as *grn* and *zfh1*. Similarly, in vMNs, *isl* (Thor and Thomas, 1997) and *Lim3* (Thor et al., 1999) work in parallel to *dfr* to specify vMN projections to the correct ventral muscles in part through the differential regulation of *beat Ic* (Certel and Thor, 2004).

We provide evidence in this work that the *eve/zfh1/grn* dMN combinatorial code of transcriptional regulators may also be required to cooperatively regulate levels of receptors in a cell-specific manner. Our data indicate that individual members of the *eve*, *grn*, *zfh1* code are differentially required or sufficient to promote expression of dMN guidance molecules. Nevertheless, their combined action leads to a more robust transcriptional response that in the case of *unc-5* is mediated through a single regulatory element (Figures 6 and 7). Importantly, this enhanced transcriptional effect is also translated into a more robust guidance response (Figure 8). Expression levels of dMN guidance molecules are likely to be very tightly regulated as indicated by the gene dosage-sensitive genetic interactions they present (Zarin et al., 2012; Figure 4). Therefore, our results strongly suggest that the combined action of these transcriptional regulators is required to attain the required levels of expression of dMN guidance molecules.

Toward a Code of Receptors for Motoneuron Guidance

While *eve* mutants show severe ISN guidance phenotypes in which all the ISNs fail to reach their dorsal muscle targets, individual mutations in the different receptors regulated by *eve* result in much milder phenotypes. These phenotypes are almost exclusively restricted to the most dorsal muscle area and have low expressivity. In contrast, we show that their combination increases the expressivity of the phenotype to 65% of the hemisegments and ISN axons stall at earlier points in their path, as they do in *eve* mutants (Fujioka et al., 2003; Landgraf et al., 1999) (Figure 3). These results indicate that these molecules act together to determine guidance of the ISN and their concerted action gives robustness to the guidance system. The coordinated action of these guidance receptors and adhesion molecules is further supported by their ability to promote CNS exit of aCC and RP2 into the muscle field and rescuing the *eve* phenotype. In this situation, we can analyze the individual contribution of each one of the molecules regulated by *eve* by reintroducing them individually or in combination in aCC and RP2. Each individual gene has little or no effect, but the combined action of all of them is able induce substantial CNS exit; in this experiment, the guidance receptors Beat-Ia and Unc-5 together can promote significant CNS exit of both motoneurons. Interestingly, they mainly induce exit where aCC and RP2 are defasciculated, joining either the ISN or the SN branch. These experiments also demonstrate the requirement for an adhesive system to allow the fasciculation of RP2 and aCC. Neither the directed guidance imparted by Unc-5 and Beat-Ia, nor the adhesive function provided by Nrg and Fas2 are alone sufficient to mediate eve's guidance activity. Only when both guidance receptors and CAMs are expressed simultaneously in aCC and RP2 motoneurons can they project out of the CNS together fasciculated in a bundle. Nevertheless, the relatively mild CNS exit phenotypes of compound mutants suggest that *eve* also regulates other genes in this process. Similarly, in the *Drosophila* eye, L3 lamina neurons require in a cell-autonomous manner the combined adhesive function of CadN and the repulsive action of Sema-1a for targeting the outer medula (Pecot et al., 2013). One might predict that other CAMs with restricted motoneuron expression, such as Connectin (Nose et al., 1992) and Fas3 (Patel et al., 1987), may provide selective fasciculation and specificity for the SNa and ISNb motor branches, respectively.

As Marc Tessier-Lavigne and Corey Goodman proposed in their landmark review:

> Thus, an individual axon might be "pushed" from behind by a chemorepellent, "pulled" from afar by a chemoattractant, and "hemmed in" by attractive and repulsive

> local cues. Push, pull, and hem: these forces appear to act together to ensure accurate guidance. (Tessier-Lavigne and Goodman, 1996)

aCC and RP2 axons will be "pushed" from behind by Netrin, "pulled" by Sidestep, and "hemmed" by Neuroglian and Fasciclin2 to establish the intersegmental nerve branch. Since this combinatorial code of guidance molecules works in a concerted way, it would only make sense that their expression is orchestrated in place and time as it is in aCC and RP2 motoneurons through the combined action of *eve*, *zfh1*, and *grn*.

EXPERIMENTAL PROCEDURES

Genetics

Fly stocks used were the following: *UAS-HA-Unc5* (Keleman and Dickson, 2001), *Unc-5*^{8}*/CyO* (Labrador et al., 2005), *UAS-beat Ia*, *beat Ia*^{C163}*/CyO*, and *beat Ia*^{3}*/CyO* (Siebert et al., 2009), *UAS–Fas2* (transmembrane, *PEST*$^{+}$ isoform) (Lin et al., 1994), *UAS-nrg*^{180} (Islam et al., 2003), and *nrg*^{3}*/FM7* (Hall and Bieber, 1997). *eve* mosaic mutants used were the following: *Df(2R)eve, RP2A/CyO; RN2-Gal4, UAS-tau-LacZ* (Fujioka et al., 2003), *UAS-eve*/TM3, *RN2-Gal4*, UAS-*tau-myc-GFP*, and UAS-*tau-myc-GFP* (Garces and Thor, 2006), *eagle-Gal4* (Dittrich et al., 1997), *RN2Gal4*, *UASmCD8GFP*, and *Df(2R)eve, RP2A, RN2Gal4, UASmCD8GFP*/SM6-TM6. Lethal mutations/insertions were kept over *FM7*, *CyO*, *TM2*, *TM3*, and *TM6* balancer chromosomes with blue balancers. Detailed genotypes are described in the Supplemental Experimental Procedures.

Cell-Specific mRNA Profiling

Wild-type and *eve* mosaic aCC and RP2 neurons were isolated from *RN2Gal4, UAS-mCD8GFP* and *Df(2R)eve, RP2A, RN2Gal4, UASmCD8GFP*/SM6-TM6 fly lines, respectively (see the Supplemental Experimental Procedures). Wild-type and *eve* mosaic embryos were aged for 8 hr at 25°C, trypsinized, and dissociated. GFP-positive neurons were purified using FACS and immediately transferred to TRIzol (Invitrogen). Total RNA was processed with the GeneChip Two-Cycle Target Labeling kit (Affymetrics) and microarray hybridized. Three biological and three technical replicates were performed for each group. Microarray output GeneChip CEL files were analyzed with the oneChannelGUI (Bioconductor) and normalized using GC-RMA algorithm. To determine differentially expressed genes between two conditions, we performed two-tailed paired t test using the Limma package from the Bioconductor project (http://www.bioconductor.org/). The p value of the moderated t test was adjusted for multiple hypotheses testing, controlling for FDR with the Benjamini-Hochberg procedure. Genes with FDR less than 0.05 (5%) and fold change greater than 1.5 were chosen for further examination. Other analyses were performed as described in detail in the Supplemental Experimental Procedures.

Immunofluorescence

Primary antibodies used were the following: anti-c-Myc 9E10 (1:50), anti-Fas2 1D4 (1:50) (Developmental Studies Hybridoma Bank), anti-HA (Covance; 1:500), anti-muscle myosin (1:50), and rabbit anti-β-gal (Cappel; 1:5,000). Alexa Fluor 488 (Molecular Probes), HRP, and Cy3 (Jackson ImmunoResearch Laboratories) conjugated anti-mouse or anti-rabbit secondary antibodies were used at 1:1,000, 1:500, and 1:500, respectively. Cy3-labeled tyramide (PerkinElmer) was used as HRP substrate. ISN projections at embryonic stage 16/17 in A2–A6 abdominal hemisegments were stained with anti-Fas2 and examined in different genetic backgrounds. Stacks of images were obtained with a Zeiss Confocal LSM700 Microscope using a 40× oil immersion objective.

RNA In Situ Hybridization

In situ hybridization to analyze the mRNA expression of different genes in aCC and RP2 dorsal motor neurons as well as eagle interneurons was performed as previously described (Labrador et al., 2005). Full-length cDNAs were PCR amplified and probes were transcribed using digoxigenin-labeled ribonucleotides. Hybridized probes were bound with anti-digoxigenin POD-conjugated Fab fragments and detected using Cy3-labeled tyramide. Anti-β-gal and anti-Myc antibodies were used for double labeling. Mutant embryos and heterozygous siblings were dissected, mounted on the same slide, and distinguished with β-galactosidase balancer chromosomes. Stacks of images were obtained as described above. Laser power and detector settings were optimized for detection of unsaturated fluorescent signal and kept constant for all the different genotypes. Fluorescence was quantified with ImageJ.

Statistics

Data are presented as mean values ± SEM. SPSS 16 software (SPSS) was used to generate histograms and determine statistical significance. For analysis of genetic interactions, Kruskal-Wallis one-way analysis of variance was used. For all other comparisons, two-independent samples t test was used. Significance levels are represented in figures with $^{**}p < 0.05$ or $^{***}p < 0.005$.

SUPPLEMENTAL INFORMATION

Supplemental Information includes Supplemental Experimental Procedures, five figures, and three tables and can be found with this article online at http://dx.doi.org/10.1016/j.neuron.2014.01.038.

ACKNOWLEDGMENTS

We would like to thank James Castelli-Gair Hombria, Barry Dickson, Herman Aberle, Luis García Alonso, Miki Fujioka, Alain Garces, and Brian McCabe for fly stocks and diverse reagents. We would also like to thank Richard Baines, Tony Southall, and Andrea Brand for sharing their unpublished data with us. This work was supported by a Principal Investigator Grant 07/IN.1/B913 and the Research Frontiers Program 08/ RFP/NSC1617 from Science Foundation Ireland (to J.-P.L.), an IRCSET Embark Initiative Postgraduate Scholarship (to A.A.Z.), and NIH Grant NS054739 (to G.J.B.).

Accepted: January 7, 2014
Published: February 20, 2014

REFERENCES

Aberle, H., Haghighi, A.P., Fetter, R.D., McCabe, B.D., Magalhães, T.R., and Goodman, C.S. (2002). wishful thinking encodes a BMP type II receptor that regulates synaptic growth in Drosophila. Neuron *33*, 545–558.

Bieber, A.J., Snow, P.M., Hortsch, M., Patel, N.H., Jacobs, J.R., Traquina, Z.R., Schilling, J., and Goodman, C.S. (1989). Drosophila neuroglian: a member of the immunoglobulin superfamily with extensive homology to the vertebrate neural adhesion molecule L1. Cell *59*, 447–460.

Bonanomi, D., and Pfaff, S.L. (2010). Motor axon pathfinding. Cold Spring Harb. Perspect. Biol. *2*, a001735.

Bonanomi, D., Chivatakarn, O., Bai, G., Abdesselem, H., Lettieri, K., Marquardt, T., Pierchala, B.A., and Pfaff, S.L. (2012). Ret is a multifunctional coreceptor that integrates diffusible- and contact-axon guidance signals. Cell *148*, 568–582.

Broihier, H.T., and Skeath, J.B. (2002). Drosophila homeodomain protein dHb9 directs neuronal fate via crossrepressive and cell-nonautonomous mechanisms. Neuron *35*, 39–50.

Broihier, H.T., Kuzin, A., Zhu, Y., Odenwald, W., and Skeath, J.B. (2004). Drosophila homeodomain protein Nkx6 coordinates motoneuron subtype identity and axonogenesis. Development *131*, 5233–5242.

Certel, S.J., and Thor, S. (2004). Specification of Drosophila motoneuron identity by the combinatorial action of POU and LIM-HD factors. Development *131*, 5429–5439.

Dasen, J.S., and Jessell, T.M. (2009). Hox networks and the origins of motor neuron diversity. Curr. Top. Dev. Biol. *88*, 169–200.

Dittrich, R., Bossing, T., Gould, A.P., Technau, G.M., and Urban, J. (1997). The differentiation of the serotonergic neurons in the Drosophila ventral nerve cord depends on the combined function of the zinc finger proteins Eagle and Huckebein. Development *124*, 2515–2525.

Doe, C.Q., Smouse, D., and Goodman, C.S. (1988). Control of neuronal fate by the Drosophila segmentation gene even-skipped. Nature *333*, 376–378.

Dudanova, I., Gatto, G., and Klein, R. (2010). GDNF acts as a chemoattractant to support ephrinA-induced repulsion of limb motor axons. Curr. Biol. *20*, 2150–2156.

Dudanova, I., Kao, T.-J., Herrmann, J.E., Zheng, B., Kania, A., and Klein, R. (2012). Genetic evidence for a contribution of EphA:ephrinA reverse signaling to motor axon guidance. J. Neurosci. *32*, 5209–5215.

Fambrough, D., and Goodman, C.S. (1996). The Drosophila beaten path gene encodes a novel secreted protein that regulates defasciculation at motor axon choice points. Cell *87*, 1049–1058.

Fujioka, M., Lear, B.C., Landgraf, M., Yusibova, G.L., Zhou, J., Riley, K.M., Patel, N.H., and Jaynes, J.B. (2003). Even-skipped, acting as a repressor, regulates axonal projections in Drosophila. Development *130*, 5385–5400.

Garces, A., and Thor, S. (2006). Specification of Drosophila aCC motoneuron identity by a genetic cascade involving even-skipped, grain and zfh1. Development *133*, 1445–1455.

Grenningloh, G., Rehm, E.J., and Goodman, C.S. (1991). Genetic analysis of growth cone guidance in Drosophila: fasciclin II functions as a neuronal recognition molecule. Cell *67*, 45–57.

Hall, S.G., and Bieber, A.J. (1997). Mutations in the Drosophila neuroglian cell adhesion molecule affect motor neuron pathfinding and peripheral nervous system patterning. J. Neurobiol. *32*, 325–340.

Harris, R., Sabatelli, L.M., and Seeger, M.A. (1996). Guidance cues at the Drosophila CNS midline: identification and characterization of two Drosophila Netrin/UNC-6 homologs. Neuron *17*, 217–228.

Herrera, E., Brown, L., Aruga, J., Rachel, R.A., Dolen, G., Mikoshiba, K., Brown, S., and Mason, C.A. (2003). Zic2 patterns binocular vision by specifying the uncrossed retinal projection. Cell *114*, 545–557.

Higashijima, S., Shishido, E., Matsuzaki, M., and Saigo, K. (1996). eagle, a member of the steroid receptor gene superfamily, is expressed in a subset of neuroblasts and regulates the fate of their putative progeny in the Drosophila CNS. Development *122*, 527–536.

Islam, R., Wei, S.-Y., Chiu, W.-H., Hortsch, M., and Hsu, J.-C. (2003). Neuroglian activates Echinoid to antagonize the Drosophila EGF receptor signaling pathway. Development *130*, 2051–2059.

Jacobs, J.R., and Goodman, C.S. (1989). Embryonic development of axon pathways in the Drosophila CNS. II. Behavior of pioneer growth cones. J. Neurosci. *9*, 2412–2422.

Kania, A., and Jessell, T.M. (2003). Topographic motor projections in the limb imposed by LIM homeodomain protein regulation of ephrin-A:EphA interactions. Neuron *38*, 581–596.

Kania, A., Johnson, R.L., and Jessell, T.M. (2000). Coordinate roles for LIM homeobox genes in directing the dorsoventral trajectory of motor axons in the vertebrate limb. Cell *102*, 161–173.

Keleman, K., and Dickson, B.J. (2001). Short- and long-range repulsion by the Drosophila Unc5 netrin receptor. Neuron *32*, 605–617.

Kolodkin, A.L., and Tessier-Lavigne, M. (2011). Mechanisms and molecules of neuronal wiring: a primer. Cold Spring Harb. Perspect. Biol. *3*, a001727.

Kramer, E.R., Knott, L., Su, F., Dessaud, E., Krull, C.E., Helmbacher, F., and Klein, R. (2006). Cooperation between GDNF/Ret and ephrinA/EphA4 signals for motor-axon pathway selection in the limb. Neuron *50*, 35–47.

Kratsios, P., Stolfi, A., Levine, M., and Hobert, O. (2012). Coordinated regulation of cholinergic motor neuron traits through a conserved terminal selector gene. Nat. Neurosci. *15*, 205–214.

Labrador, J.P., O'keefe, D., Yoshikawa, S., McKinnon, R.D., Thomas, J.B., and Bashaw, G.J. (2005). The homeobox transcription factor even-skipped regulates netrin-receptor expression to control dorsal motor-axon projections in Drosophila. Curr. Biol. *15*, 1413–1419.

Landgraf, M., and Thor, S. (2006). Development of Drosophila motoneurons: specification and morphology. Semin. Cell Dev. Biol. *17*, 3–11.

Landgraf, M., Roy, S., Prokop, A., VijayRaghavan, K., and Bate, M. (1999). even-skipped determines the dorsal growth of motor axons in Drosophila. Neuron *22*, 43–52.

Layden, M.J., Odden, J.P., Schmid, A., Garces, A., Thor, S., and Doe, C.Q. (2006). Zfh1, a somatic motor neuron transcription factor, regulates axon exit from the CNS. Dev. Biol. *291*, 253–263.

Lin, D.M., Fetter, R.D., Kopczynski, C., Grenningloh, G., and Goodman, C.S. (1994). Genetic analysis of Fasciclin II in Drosophila: defasciculation, refasciculation, and altered fasciculation. Neuron *13*, 1055–1069.

Marqués, G., Bao, H., Haerry, T.E., Shimell, M.J., Duchek, P., Zhang, B., and O'Connor, M.B. (2002). The Drosophila BMP type II receptor Wishful Thinking regulates neuromuscular synapse morphology and function. Neuron *33*, 529–543.

Mitchell, K.J., Doyle, J.L., Serafini, T., Kennedy, T.E., Tessier-Lavigne, M., Goodman, C.S., and Dickson, B.J. (1996). Genetic analysis of Netrin genes in Drosophila: Netrins guide CNS commissural axons and peripheral motor axons. Neuron *17*, 203–215.

Nose, A., Mahajan, V.B., and Goodman, C.S. (1992). Connectin: a homophilic cell adhesion molecule expressed on a subset of muscles and the motoneurons that innervate them in Drosophila. Cell *70*, 553–567.

Odden, J.P., Holbrook, S., and Doe, C.Q. (2002). Drosophila HB9 is expressed in a subset of motoneurons and interneurons, where it regulates gene expression and axon pathfinding. J. Neurosci. *22*, 9143–9149.

Patel, N.H., Snow, P.M., and Goodman, C.S. (1987). Characterization and cloning of fasciclin III: a glycoprotein expressed on a subset of neurons and axon pathways in Drosophila. Cell *48*, 975–988.

Pecot, M.Y., Tadros, W., Nern, A., Bader, M., Chen, Y., and Zipursky, S.L. (2013). Multiple interactions control synaptic layer specificity in the Drosophila visual system. Neuron *77*, 299–310.

Pym, E.C.G., Southall, T.D., Mee, C.J., Brand, A.H., and Baines, R.A. (2006). The homeobox transcription factor Even-skipped regulates acquisition of electrical properties in Drosophila neurons. Neural Dev. *1*, 3.

Sánchez-Soriano, N., and Prokop, A. (2005). The influence of pioneer neurons on a growing motor nerve in Drosophila requires the neural cell adhesion molecule homolog FasciclinII. J. Neurosci. *25*, 78–87.

Siebert, M., Banovic, D., Goellner, B., and Aberle, H. (2009). Drosophila motor axons recognize and follow a Sidestep-labeled substrate pathway to reach their target fields. Genes Dev. *23*, 1052–1062.

Sink, H., Rehm, E.J., Richstone, L., Bulls, Y.M., and Goodman, C.S. (2001). sidestep encodes a target-derived attractant essential for motor axon guidance in Drosophila. Cell *105*, 57–67.

Tessier-Lavigne, M., and Goodman, C.S. (1996). The molecular biology of axon guidance. Science *274*, 1123–1133.

Thor, S., and Thomas, J.B. (1997). The Drosophila islet gene governs axon pathfinding and neurotransmitter identity. Neuron *18*, 397–409.

Thor, S., Andersson, S.G., Tomlinson, A., and Thomas, J.B. (1999). A LIM-homeodomain combinatorial code for motor-neuron pathway selection. Nature *397*, 76–80.

Tsuchida, T., Ensini, M., Morton, S.B., Baldassare, M., Edlund, T., Jessell, T.M., and Pfaff, S.L. (1994). Topographic organization of embryonic motor neurons defined by expression of LIM homeobox genes. Cell *79*, 957–970.

Zarin, A.A., Daly, A.C., Hülsmeier, J., Asadzadeh, J., and Labrador, J.-P. (2012). A GATA/homeodomain transcriptional code regulates axon guidance through the Unc-5 receptor. Development *139*, 1798–1805.

Zarin, A.A., Asadzadeh, J., and Labrador, J.-P. (2014). Transcriptional regulation of guidance at the midline and in motor circuits. Cell. Mol. Life Sci. *71*, 419–432.